Species-Specific Growth Models Inform Sustainable Management of Rhizophora mangle in the Colombian Caribbean Wetlands Ecology and Management

David Valderrama

dvalderramaca@unal.edu.co

Universidad Nacional de Colombia, sede Medellín

Jaime Polanía

Universidad Nacional de Colombia, sede Medellín

Valeria Aguiar

Universidad Nacional de Colombia, sede Medellín

Sergio Orrego

Universidad Nacional de Colombia, sede Medellín

Research Article

Keywords: Mangrove silviculture, tree-rings, ontogenic traits, silvicultural parameters

Posted Date: December 4th, 2025

DOI: https://doi.org/10.21203/rs.3.rs-8245794/v1

Additional Declarations: No competing interests reported.

Version of Record: A version of this preprint was published at Wetlands Ecology and Management on April 27th, 2026. See the published version at https://doi.org/10.1007/s11273-026-10139-7.

Abstract

Mangrove ecosystems provide crucial ecological services but face threats from climate change and unsustainable resource use. This highlights the need for science-based forest management initiatives. Cispatá Bay, located in the Colombian Caribbean, hosts the country's only mangrove under a regulated sustainable use model. Yet, current management guidelines rely on generalized silvicultural criteria, such as a uniform minimum logging diameter (MLD) of 10 cm and a 14-year cutting cycle (CC), which do not reflect species-specific growth dynamics, potentially compromising sustainability. This study aims to improve sustainable forest management in Cispatá Bay by developing species-specific growth models for *Rhizophora mangle*, a dominant and heavily harvested species. We introduce a novel methodological framework for sustainable forest management in mangrove ecosystems, integrating dendrochronology and biometric modeling to derive ecological management parameters. We combined tree-ring data from 26 dead individuals with forest inventory measurements and applied nonlinear mixed-effects modeling, accounting for autocorrelation and growth eccentricity. The resulting models yielded biologically meaningful ontogenetic traits, including a maximum mean diameter (A_{max}) of 40.35 cm, a weighted average growth rate (WAGR) of 0.42 cm year^{-1}, a lifespan (t_{span}) of 95.12 years, and a halflife ($t_{0.5}$) of 41.09 years. Additionally, we estimated an MLD of 24 cm and a CC of 20 years—both substantially higher than current thresholds. These findings suggest that continued application of generalized metrics may compromise forest regeneration, reduce volume recovery, and undermine long-term sustainability. By integrating dendrochronological techniques with biometric modeling, this research provides a replicable framework for evidence-based forest governance in mangroves.

1. Introduction

Mangroves provide a wide range of ecosystem services, including carbon sequestration, water regulation, and protection against extreme climatic events such as floods and hurricanes (Bimrah et al. 2022; Mitra 2020). They also support local livelihoods by supplying essential resources for food, fuel, and construction (Hussain and Badola 2010; Palacios and Cantera 2017). Despite their ecological and socioeconomic importance, mangroves are increasingly threatened by climate change, urban expansion, and high deforestation rates (Bhowmik et al. 2022; Kumari and Pathak 2023). Ensuring their persistence requires conservation and forest management strategies grounded in robust silvicultural parameters that enable sustainable resource use.

Sustainable forest management in tropical ecosystems relies on accurate information about structural and dynamic parameters such as diameter, height, volume growth, age, and regeneration processes (Schöngart 2008). Traditionally, tropical tree growth has been assessed through periodic measurements in permanent sampling plots (Dauber et al. 2005; Vanclay 1994) or through dendrochronological techniques that reconstruct annual growth patterns from tree rings (Andrade et al. 2019; Conde et al. 2024; Inga and del Valle 2017; Martínez et al. 2025; Xu et al. 2014). Dendrochronology is generally less expensive and time-consuming than long-term plot monitoring and offers higher temporal precision, providing continuous annual records that span the entire lifespan of individual trees (Inga and del Valle 2017). Given the need for reliable long-term growth and age data in mangrove ecosystems (Chowdhury et al. 2023a), dendrochronology presents a particularly efficient and accessible approach for species that form distinct annual growth rings.

Mangrove species' growth is influenced by various environmental drivers, among which salinity is the primary limiting factor (Lovelock et al. 2016). Salinity in mangrove environments fluctuates seasonally in response to rainfall and freshwater inflows; during dry periods, reduced freshwater input increases salinity, imposing additional energetic costs that constrain growth (Kodikara et al. 2017; Lovelock et al. 2016). These fluctuations are recorded in the anatomical structure of growth rings (Chowdhury et al. 2023b). Annual growth rings have been observed in several mangrove species, including *Excoecaria agallocha* (Siddique et al. 2021), *Laguncularia racemosa* (Estrada et al. 2008), *Sonneratia apetala* (Chowdhury et al. 2008), *Rhizophora mangle* (Menezes et al. 2003; Ramírez-Correa et al. 2010; Souza et al. 2016), R. *mucronata* (Verheyden et al. 2004), *Xylocarpus granatum* (Chowdhury et al. 2023b), and *Heritiera fomes* (Chowdhury et al. 2008), among others.

Between 1938 and 1945, the diversion of the Sinú River allowed seawater to intrude into Cispatá Bay, creating favorable conditions for mangrove colonization in areas previously used for rice cultivation (Suárez 2004). Since then, the local economy has become heavily dependent on mangrove resources, particularly timber from *R. mangle*. Approximately 94% of the local population relies on *R. mangle* wood as a primary source of fuel for cooking and heating (Dupont et al. 2025), with additional uses including local construction and commercialization (CVS and INVEMAR 2010). However, intensive extraction has led to significant ecological changes in mangrove populations. In response, the Corporación Autónoma Regional de los Valles del Sinú y del San Jorge (CVS) and the Instituto de Investigaciones Marinas y Costeras (INVEMAR) launched an Integrated Management Plan (IMP) in 2008 to promote the sustainable use of mangrove resources (CVS and INVEMAR 2010).

The IMP was developed using forest inventory data collected from permanent sampling plots, which provided valuable insights into forest structure, composition, growth, and mortality. Nevertheless, some measurements—such as tree height—were recorded with limited precision (rounded to the nearest meter), introducing potential bias into structural analyses. Using these data, the plan established a 14-year cutting cycle (CC) for *R. mangle*. However, other critical silvicultural parameters, including the minimum logging diameter (MLD), were not derived from species-specific ecological data but instead followed national legislation that applies a uniform MLD of 10 cm to all tree species across Colombia (República de Colombia 1996). Under this framework, timber extraction was organized using a polycyclic system that divided Cispatá Bay into 14 sectors, each harvested sequentially while the remaining sectors regenerated.

This reliance on generalized regulations reflects a broader issue in tropical forest governance. Government-mandated criteria often overlook interspecific variability, resulting in either overexploitation or underutilization of forest resources (Andrade et al. 2019; Conde et al. 2024; Dauber et al. 2005; López et al. 2013). Given the high diversity of tropical forests, such uniform prescriptions are ecologically inadequate. Although some forest management systems have begun adopting species-specific parameters (De Ridder et al. 2013; Schöngart 2008), this approach remains rare in mangrove management.

Applying generalized silvicultural criteria to *R. mangle* in Cispatá Bay, without accounting for its species-specific growth dynamics, leads to three possible outcomes: (i) the existing parameters align with the species' ecological requirements, ensuring sustainability; (ii) the prescribed MLD and/or CC exceed the species’ needs, resulting in underutilization of resources; or (iii) the metrics fall below ecological thresholds, compromising sustainability and impairing ecosystem functionality.

This study introduces a novel methodological framework for sustainable mangrove forest management. We analyzed the diameter, height, and volume growth of *R. mangle* using tree-ring data and forest inventory measurements. Through biometric modeling and growth analysis, we derived reliable ontogenetic traits and silvicultural parameters to inform evidence-based management practices for *R. mangle* in Cispatá Bay.

2. Material and methods

2.1. Study area

The study was conducted in Cispatá Bay (9°23’17”N, 75°50’55”W), located in the Colombian Caribbean region of South America (Fig. 1). The study area exhibits a mean annual temperature of 27.87 ± 0.38°C and an average annual precipitation of 1,266.76 ± 210.14 mm. A distinct dry season extends from December to March, during which monthly rainfall remains below 40 mm. The wet season occurs from May to November, with monthly precipitation typically exceeding 110 mm.

Cispatá Bay is part of the IMP for Cispatá, La Balsa, Tinajones, and adjacent ecosystems. The plan encompasses a total area of 27,171 ha, of which 8,571 ha are mangrove forests (CVS and INVEMAR 2010). These mangroves are characterized by elevated salinity and periodic inundation—conditions that strongly influence species composition. *R. mangle* is the

dominant species and the first to colonize the ecotone between marine and terrestrial environments, followed by *Avicennia germinans* and *L. racemosa*.

2.2. Forest inventories

The forest inventories were established with the development of the IMP (CVS and INVEMAR 2010), and data from seven transects of fringe mangroves in Cispatá Bay were provided by INVEMAR. Due to substantial variability in topographical and hydrological conditions (e.g., the presence of streams and lagoons), continuous sampling was not feasible, resulting in transect areas ranging from 0.45 to 1.46 ha. Within each transect, 10 × 10 m plots were delineated to identify species and to measure tree diameter and height for all individuals with a diameter greater than 3.5 cm. For *R. mangle*, diameter was measured 30 cm above the highest aerial root, in accordance with its characteristic stilt-root structure, whereas for *A. germinans* and *L. racemosa*, diameter at breast height (DBH) was recorded.

2.3. Sampling and tree-ring analyses

Due to the complex wood anatomy of mangrove species, including the occurrence of false or wedging rings (Chowdhury et al. 2016, 2024; Rahman et al. 2020), cross-sections were collected instead of increment cores. Because tree harvesting is regulated under the IMP, 26 cross-sections were obtained from dead or felled *R. mangle* trees, sampled as close to the base as possible but above the aerial roots. The felled trees were selected using size and visible condition, prioritizing individuals with diameters greater than 10 cm that still retained foliage or showed no visible signs of decay. All samples were oven-dried at 60°C for four days. To enhance ring visibility, each sample was polished using a sanding machine with progressively finer abrasive paper (grits 60–600). The prepared samples were then processed at the Laboratorio Bosques y Cambio Climático of the Universidad Nacional de Colombia, where they were digitized at a resolution of 2400 dpi using an Epson 10000XL scanner.

Growth rings in *R. mangle* were delimited using variations in vessel density (Fig. S1). Ring-width measurements (radial increments) were obtained using the Coorecorder software (Cybis Elektronik and Data AB n.d.-a), and a composite reference chronology was developed with Cdendro (Cybis Elektronik and Data AB n.d.-b). Subsequent analyses of ring-width data were conducted in the R environment (R Core Team 2024) using the dplR package (Bunn et al. 2022).

Because the material originated from dead and fallen trees, a decay classification system was applied as follows: (1) no visible decay; (2) minor decay; (3) moderate decay, making ring delimitation difficult; (4) advanced decay, permitting ring measurement in only one radius; and (5) severe decay, rendering the sample unsuitable for analysis (Fig. 2).

2.4. Growth modelling

The tree diameter was calculated as twice the radius, with the radius determined from the cumulative ring width. However, this value may be inaccurate when the pith does not coincide with the geometric center of the cross-section (Chowdhury et al. 2024; Giraldo and del Valle 2011). To address this, an eccentricity correction factor was applied to each measurement following Giraldo and del Valle (2011):

$$RW_c = \frac{\frac{P_c}{2\pi}}{r_m} \bullet RW_m$$

1

,

where RW_c is the corrected ring width, P_c is the perimeter of the sample, r_m is the radius length at which the ring widths were measured, and RW_m is the measured ring width.

Although two radii were measured for most samples, only one was randomly selected for diameter growth modeling, while the second radius was used for statistical validation. In samples where only one radius was available, that measurement

was included directly in the modeling dataset.

Diameter growth was modeled using the von Bertalanffy growth equation (von Bertalanffy 1934), which describes organism growth as the balance between anabolic and catabolic processes. In the context of tree growth, anabolism corresponds to photosynthetic production, whereas catabolism represents respiratory consumption:

$$\frac{dD}{dt} = \eta D^m - \gamma D,$$

2

where $\frac{dD}{dt}$ denotes the growth rate, *D* is the diameter, *t* is the age, and ηD^m and γD are the photosynthesis and respiration rates, respectively.

Since tree-ring data provide measurements beginning from the first year of growth, a diameter of zero was assumed at *t* = 0. Integrating Eq. (2) under these conditions yields:

$$D(t) = \left(\frac{\eta}{\gamma}\right)^{\frac{1}{1-m}} \left(1 - e^{-\gamma (1-m)t}\right)^{\frac{1}{1-m}}.$$

3

A nonlinear mixed-effects (NLME) approach was applied to model Eq. (3). The photosynthetic parameters (η , m) were treated as random effects, while the respiration parameter (γ) was modeled as a fixed effect common to all trees, following Martínez et al. (2025). The general expression of Eq. 3 within the NLME framework can be formulated as follows:

$$D_{ij} = f\left(t_{ij}, \phi_{ij}\right) + \epsilon_{ij}\, i = 1, \ldots, M; j = 1, \ldots, n_i$$

4

,

where f is a nonlinear response function with respect to ϕ_{ij}, t_{ij} is the diameter of observation j and tree i, M is the number of trees, and n_i is the number of observations within the tree *I*, ϵ_{ij} is the unexplained error. The parameter vector for a single observation is defined in matrix form as follows :

$$\phi_{ij} = A_{ij}\beta + B_{ij}b_i,$$

5

where β is the vector of fixed parameters, b_i is the vector of random parameters, and A_{ij} and B_{ij} are the design matrices that link the fixed and random effects to the nonlinear parameters ϕ_{ij}.

Because tree-ring data consist of repeated measurements from the same individual, they may exhibit temporal dependence or autocorrelation (Mehtätalo and Lappi 2020). Therefore, after estimating model (4), we examined the residual correlation structure and tested several autoregressive integrated moving average (ARIMA) specifications to account for potential autocorrelation among observations (Martínez et al. 2025).

To estimate height growth, 80% of the forest inventory data were used to fit an allometric diameter-height model, while the remaining 20% were reserved for model validation. The relationship between diameter and height was described using a two-parameter Michaelis-Menten equation, a nonlinear theoretical model originally developed for enzyme kinetics (Michaelis and Menten 1913; Srinivasan 2022), but also widely applied in tropical forests to characterize diameter-height

allometry (Conde et al. 2024; Schöngart 2008). In this model, the parameters represent the mean maximum tree height and the rate at which it is approached. The Michaelis-Menten equation can be written as follows:

$$H = \frac{\alpha}{1 + \left(\frac{\beta}{DBH}\right)}$$

6

,

where H denotes total height, DBH denotes diameter at breast height, α represents the asymptote (mean maximum height), and β is the parameter defining the rate of approach to the asymptote.

Because inventory data is collected from plots within transects, a two-level, nested, mixed-effects nonlinear model (NLME) was used to fit Eq. 6:

$$H_{ijk} = f\left(D_{ijk}, \phi_{ijk}\right) + \epsilon_{ijk}\, i = 1, \ldots, M; j = 1, \ldots, M_i; k = 1, \ldots, n_{ij,}$$

7

where f is a nonlinear response function with respect to ϕ_{ijk}, D_{ijk} is the diameter of tree k in plot j and transect i, M is the number of transects, m_i is the number of plots within transect *i*, n_{ij} is the number of trees, and ϵ_{ijk} is the unexplained residual error.

Model performance was assessed by testing all possible combinations of random parameters, using the Akaike Information Criterion (AIC), Bayesian Information Criterion (BIC), and log-likelihood (logLik) as model selection metrics. The model exhibiting the lowest AIC and BIC values and the highest logLik was selected as the best-fitting model. Subsequently, the diameter values derived from the tree-ring data were substituted into Eq. 6 to estimate the height of each tree throughout its lifespan. All models in this study were fitted using maximum likelihood estimation (MLE) implemented in the nlme package (Pinheiro et al. 2021) within the R software environment (R Core Team 2024).

The presence of heteroscedasticity was assessed graphically for both diameter-growth and diameter-height models. When evidence of heteroscedasticity was detected, variance functions were incorporated into the models to stabilize residual variance, including the power function of the covariate (*VarPower*), the exponential function of the covariate (*VarExp*), and different variances among analytical units (e.g., trees, transects) using *VarIdent* structures. Additionally, the assumption of normality was evaluated through visual inspection of residual frequency histograms.

We evaluated the model's fit using the validation dataset. The following measurements of bias, precision, and performance, as proposed by Vanclay (1994), were calculated:

Average bias (AB):

$$AB = \frac{\sum_{i=1}^{n}(y_i - \widehat{y_i})}{n}$$

8

,

where y_i is the *ith* observation, $\widehat{y_i}$ is the *ith* predicted value of the model, and *n* is the number of observations of the validation dataset

To measure precision, the mean absolute error (MAE) was calculated:

$$MAE = \frac{\sum_{i=1}^{n} |y_i - \widehat{y_i}|}{n}$$

9

.

The model efficiency (ME) was also calculated:

$$ME = 1 - \frac{\sum_{i=1}^{n} (y_i - \widehat{y_i})^2}{\sum_{i=1}^{n} (y_i - \bar{y})^2}$$

10

,

where $\bar{y}$ is the response variable's average.

EM is analogous to R^2 for nonlinear regression. A perfect fit is indicated by a value of one, while negative values represent a poor fit of the model.

Annual tree volume was estimated by applying a form factor of 0.657, previously reported for *R. mucronata* (Roberts and Ruara 1967). This species belongs to the same genus as *R. mangle* and exhibits a highly similar stem architecture, making the form factor an appropriate proxy for the studied species. The annual volume was estimated as follows:

$$V_t = \pi \ (\frac{D_t}{2})^2 \bullet \ H_t \bullet \ f,$$

11

where $V_t,\ D_t,$ and H_t is the volume, diameter, and height at time *t*, respectively, and f is the form factor.

We calculated the current and mean annual increment of the volume (CAI_V and MAI_V) as follows:

$$CAIv_t = CV_{t+1} - CV_t,$$

12

$$MAIv_t = \frac{CV_t}{t}$$

13

,

where CV_t represents the cumulative volume at time *t*.

2.5. Ontogenic traits and silvicultural parameters

Based on the diameter growth model, several ontogenic traits proposed by Inga and del Valle (2017) were calculated. The maximum mean diameter (A_{max}), represents the asymptote of diameter in centimeters and corresponds to the theoretical upper limit of *D* as time (t) approaches infinity:

$$A_{max} = (\frac{\eta}{\gamma})^{\frac{1}{1-m}}$$

14

.

The weighted absolute growth rate (WAGR) is an age-independent estimation of the growth rate throughout the lifespan of the species:

$$WAGR = \frac{(\frac{\eta}{\gamma})^{\frac{1}{1-m}} \bullet \ \gamma \ \bullet \ (1-m)}{2 \bullet \ (m+1)}$$

15

.

Lifespan (t_{span}) is the time in years required for the population to reach A. It is calculated as the quotient of A and $WAGR$:

$$t_{span} = \frac{2 \bullet \ (m+1)}{\gamma \ \bullet \ (1-m)}$$

16

.

Half-life ($t_{0.5}$) represents the time in years needed to reach half of A_{max}:

$$t_{0.5} = -\frac{ln\left(1-(0.5)^{1-m}\right)}{\gamma\,(1-m)}$$

17

.

The MLD and CC were determined following the Growth-Oriented Logging (GOL) concept proposed by Schöngart (2008). According to this concept, trees should be harvested at an age between the maximum values of the CAI_V and MAI_V to optimize the species' growth potential. Harvesting trees before or after this interval results in suboptimal resource use and reduced yield efficiency. The MLD is defined as the diameter reached by the species at the age corresponding to the maximum CAI_V.

The CC was calculated as the average time required for the species to grow from one diameter class of 10 cm to the next:

$$CC = \frac{age_{MLD}}{MLD \bullet \ 0.1}$$

18

.

3. Results

3.1. Forest structure

The total tree abundance in Cispatá Bay was estimated at 1,014.89 ± 300.66 individuals ha^{-1}, of which 888.62 ± 211.75 individuals ha^{-1} (88%) corresponded to *R. mangle* trees (diameter $\geq$ 3.5 cm). The abundance of *R. mangle* followed a reverse J-shaped distribution across diameter classes (Fig. 3a). The average diameter and height were 11.8 ± 9.6 cm and 9.6 ± 3.2 m, respectively. The species had a volume stock of 129.15 m^3 ha^{-1}, with 95% exceeding the current MLD of 10 cm applied in Cispatá Bay. The volume distribution by diameter class was unimodal, peaking between 30–40 cm, with sharp declines in both smaller and larger classes (Fig. 3b).

3.2. Tree-ring data and growth trajectories

Twenty-two samples exhibited moderate or lower decay, allowing measurement of two radii per sample, while two samples with advanced decay allowed measurements from only one radius. Two severely decayed samples were excluded from the analysis (Table S1)

The ages of sampled trees ranged from 30 to 92 years. Growth trajectories revealed a clear growth depensation pattern (i.e., increasing intraspecific variability over time; Fig. S2). Applying the eccentricity correction factor significantly modified the growth trajectories, reducing some of the observed variability (Fig. S2). For example, the two uncorrected diameters calculated for the tree Z6 were 39.0 cm and 50.6 cm, while the corrected circumference-based value was 33.7 cm (Table S1). After correction, the 26 analyzed trees exhibited diameters ranging from 12.6 to 42.6 cm (Table S1).

3.3. Growth models

The von Bertalanffy (1934) equation, combined with a mixed-effects modeling approach and autocorrelation correction, provided an excellent fit for *R. mangle* diameter growth (Fig. 4). Model validation indicated low bias (AB = 0.005), high precision (MAE = 0.15), and strong performance (ME = 99.95%). Before incorporating the correlation structure, the residuals displayed a stochastic autocorrelation trend, which was effectively corrected using an ARIMA(1, 1, 0) specification (Fig. S3). Residual histograms indicated normal distribution, and homogeneous variance was confirmed without requiring an additional variance function (Fig. S3). All parameters were significant at the 99% confidence level (Table 1). Parameters η and m varied among trees from 0.31 to 0.52 and 0.47 to 0.63, respectively (Table S2).

Table 1
Estimated parameters for diameter growth and diameter-height models for R. mangle

Model	Fixed effects			Random effects		Correlation structure	Variance structure
Diameter growth	η	m	γ	σ_η	σ_m		
	0.376***	0.571***	0.077***	0.061	0.048	ARIMA(1,1,0); $\varphi : 0.28$***	VarConst
Diameter - Height	α	β	-	$\sigma_{\alpha i}/\sigma_{\alpha j}$	$\sigma_{\beta i}/\sigma_{\beta j}$	-	VarPower; $\delta : 1.32$
	15.593***	7.535***	-	1.215/1.118	0.909/1.838		

σ_η and σ_m are the standard deviations of the random parameters η y m of the diameter growth model, respectively; $\sigma_{\alpha i}$ y $\sigma_{\beta i}$ are the standard deviations at transect level of the random parameters α and β, while $\sigma_{\alpha j}$ y $\sigma_{\beta j}$ are the standard deviations at plot level; ARIMA (p,d,q): Autoregressive Integrated Moving Average model as the correlation structure, where p, d, and q are the order of the autoregressive polynomial (AR), differencing, and moving average (MA) polynomials, respectivel; φ are the estimated parameters of the AR structure. VarConst refers to constant variance among the residuals, while VarPower refers to the power of variance function which accounts for increase in variance of the residuals as fitted values increases. δ is the parameter of the variance function.

Substantial variability was observed in the diameter-height relationship (Fig. 5). The model treating α and β as random parameters demonstrated the best fit, based on the lowest AIC and BIC and the highest Loglik (Table 2, A.3), and was therefore selected to model diameter-height allometry (Fig. 5). The final model showed AB = 0.066, ME = 68.2%, and MAE = 1.28 (Table 2), with all parameters statistically significant at the 99% confidence level (Table 1). The initial model exhibited increasing variance with diameter, which was successfully addressed by adding a power variance function (Fig. S4). The residuals were normally distributed (Fig. S4).

Table 2
Validation parameters for the diameter growth and diameter-height models

Model	AB	MAE	ME (%)
Diameter growth	0.005	0.147	99.956
Diameter - Height	0.066	1.278	68.206
AB: average bias; MAE: mean absolute error; ME: model efficiency			

Based on the CAI_V curve, *R. mange* reached its maximum (0.015 m^3 $year^{-1}$) at 49 years, while the maximum MAI_V occurred at 81 years (0.009 m^3 $year^{-1}$) (Fig. 6).

3.4. Ontogenic traits and silvicultural parameters

According to the diameter growth model, the estimated parameters were: A_{max} = 40.09 cm, WAGR = 0.42 cm $year^{-1}$, t_{span} = 95.12 years, and $t_{0.5}$ = 41.09 years (Table 3). Using the volume estimates, the optimal harvesting period was determined to occur between 49 and 81 years, with a CC of 20 years. During this period, an average tree would reach a diameter of 24–34 cm. The specific MLD for *R. mangle* was estimated at 24 cm, typically achieved at 49 years—more than double the current legal MLD of 10 cm, which is reached at 24 years (Fig. 6 and Table 3).

Table 3
Ontogenic traits and silvicultural parameters derived from growth models for Rhizophora mangle's population in Cispatá Bay.

Parameter	Value
Amax	40.35 cm
WAGR	0.42 cm $year^{-1}$
t_{span}	95.12 years
$t_{0.5}$	41.09 years
MLD	24 cm
Age_{MLD}	49 years
$Age_{D=10}$	24 years
CC	20 years
Amax: maximum mean diameter or the estimated asymptote for the diameter model; WAGR: weighted absolute growth rate; t_{span}: lifespan; $t_{0.5}$: half-life; MLD: minimum logging diameter; Age_{MLD}: age at which the minimum logging diameter is reached; $Age_{D=10}$: age at which the current minimum logging diameter used in Cispatá Bay (10 cm) is reached; CC: cutting cycle.	

4. Discussion

This study examined the sustainable management of *R. mangle*, a dominant and heavily harvested mangrove species in the Colombian Caribbean. We combined tree-ring and forest inventory data to model diameter, height, and volume growth, from which ontogenic traits and silvicultural parameters were derived. Although similar approaches have been applied in other tropical forests, this represents the first application in mangrove ecosystems.

4.1. Forest structure

Cispatá Bay showed a total tree abundance of 1014.89 ± 300.66 individuals ind ha^{-1} with diameter > 3.5 cm. When considering individuals with a diameter > 5 cm, abundance was lower than that of well-preserved fringe mangroves in the Colombian Caribbean (Urrego et al. 2009) but comparable to sites under intensive wood extraction and degradation (Urrego et al. 2014). The inverse J-shaped distribution of *R. mangle* abundance observed here is consistent with other fringe mangrove ecosystems (Urrego et al. 2014), reflecting high regeneration rates driven partly by gap formation following harvesting, which facilitates seedling establishment (Duke 2001; Sherman et al. 2000; Urrego et al. 2014).

4.2. Tree-ring sampling and growth trajectories

The use of cross-sections from felled or naturally dead trees enabled reliable tree-ring analyses, allowing precise estimates of diameter growth, ontogenetic traits and silvicultural parameters for *R. mangle*. While tree-ring studies of dead trees are common in extratropical regions (Bocking et al. 2017; Speer 2010), they are rarely applied in tropical settings due to indistinct rings and high decomposition rates (Fichtler et al. 2003; Groenendijk et al. 2015). Mangrove environments, however, are saline and anoxic, which retard decomposition, making this method feasible (Ouyang et al. 2017; Simpson et al. 2023). Frequent disturbances such as storms and deforestation (Asari et al. 2021; Chowdhury et al. 2017) also yield recently fallen trees suitable for sampling. This study, therefore, supports the use of non-destructive sampling in mangroves where timber extraction is limited.

We observed substantial variability in diameter growth trajectories, consistent with growth depensation reported for *R. mangle* in Brazil (Menezes et al. 2003) and for many tropical species (Andrade et al. 2019; Brienen et al. 2010; Free et al. 2014; Martínez et al. 2025). Such intraspecific variation arises from persistent environmental effects, periods of suppression and release, autocorrelation, and genetic diversity (Brienen et al. 2010; Brienen and Zuidema 2006; Martínez et al. 2025). Importantly, we demonstrated that neglecting growth eccentricity can substantially bias diameter estimates and model outputs (Fig. S2), with over- or underestimation of up to 50% and 30%, respectively (Table S1). Similar findings were reported by Visser et al. (2023), who showed that ignoring eccentricity can distort basal area increment estimates by up to 55%. Eccentric growth—often linked to wind exposure, crown asymmetry, competition, and slope— is seldom considered in tropical growth studies (Brienen and Zuidema 2006; Conde et al. 2024; Free et al. 2014; Šilhán 2019). Measuring multiple radii (Visser et al. 2023) or applying perimeter-based correction factors (Gebrekirstos et al. 2008; Giraldo and del Valle 2011) can effectively minimize these errors, as implemented in this study.

4.3. Growth modeling

The von Bertalanffy (1934) model, applied through an NLME framework, effectively described *R. mangle*'s diameter growth and variability. Model performance was further improved by incorporating an ARIMA specification, which captured the species' growth autocorrelation; failing to do so could otherwise bias long-term estimates by underestimating growth in fast-growing trees (Brienen et al. 2006). The estimated m parameter was biologically consistent with the metabolic theory underlying the model (Richards 1959), with values between 0.48 and 0.63. This allowed meaningful interpretation of the calculated η (0.376) and γ (0.077) parameters as proportional coefficients of photosynthesis and respiration (Martínez et al. 2025), offering insights into species physiology. *R. mangle* exhibits ontogenetic shifts in light requirements, showing shade tolerance in early stages and accelerated growth under canopy openings (da Silva et al. 2015; Ellison and Farnsworth 1993). The estimated η (0.376) for *R. mangle* closely matches that for *Humiriastrum procerum* as shade-tolerant in the Chocó biogeographic region (η = 0.384) and is substantially lower than *Apeiba macropetala* (η = 0.999), a fast-growing heliophyte in the same region (Martínez et al. 2025).

The diameter–height allometric model derived from inventory data displayed considerable variability, unlike the stronger fit (R^2 = 0.85) reported by Méndez-Alonzo et al. (2015) for *R. mangle* in La Mancha Lagoon, Mexico. Variations in soil salinity, phosphorus availability, and light conditions largely explain such differences between sites (Cisneros-de la Cruz et al. 2018). The higher variability in this study may also stem from measurement error due to the 1-meter precision of the instrument used for height estimation.

4.4. Ontogenic traits and silvicultural parameters

The growth models enabled the calculation of ontogenic traits and volume growth over the species' lifespan, supporting the derivation of silvicultural parameters under the GOL concept. While several studies have analyzed similar parameters in tropical forests (Andrade et al. 2019; Conde et al. 2024; Inga and del Valle 2017; Lisboa et al. 2025; Martínez et al. 2025; Schöngart 2008), this represents the first such assessment in mangroves. We calculated an A_{max} of 40.09 cm, WAGR of 0.42 cm y^{-1}, t_{span} of 95.12 years, and $t_{0.5}$ of 41.09 years. The maximum diameter may be influenced by salinity, temperature, and storm events (Lovelock et al. 2016). For instance, dwarf *R. mangle* populations dominate in subtropical Florida (Coronado-Molina et al. 2004), whereas mangroves in the Colombian Pacific, considered the tallest in the Americas, can reach diameters of 96.7 cm (Castellanos-Galindo et al. 2021). Our A_{max} value thus represents a theoretical population mean, not an upper physical limit. The highest-growth individuals (Table S2) reached diameters consistent with the largest trees in Cispatá Bay (56 cm). The WAGR estimated here agrees with radial increment rates (0.13–0.33 cm y^{-1}) reported for Brazil (Menezes et al. 2003) and provides a more age-independent indicator of performance than absolute growth (Inga and del Valle 2017). The lifespan estimated for *R. mangle* was shorter than the 250-year maximum reported by Chen and Twilley (1998) for Mexico, likely reflecting smaller diameters in our population. To our knowledge, this is the first study to estimate $t_{0.5}$ for *R. mangle*.

4.5. Management implications

The MLD and CC are key criteria for sustainable tropical forest management. We calculated an MLD of 24 cm, achieved at 49 years—more than double the 10 cm currently applied in Cispatá Bay, which is reached at 24 years of age. Similar discrepancies have been reported when the GOL-based parameters are used (Andrade et al. 2019; Conde et al. 2024; Schöngart 2008). The existing 14-year CC defined in the local management plan differs significantly from our 20-year estimate based on tree-ring data. This difference reflects the higher temporal precision of dendrochronological methods, which account for growth autocorrelation and individual variability (Brienen and Zuidema 2006; Inga and del Valle 2017; Martínez et al. 2025).

The current silvicultural parameters used in Cispata Bay may not be optimal for ensuring long-term sustainability and mangrove regeneration. A low MLD jeopardizes regeneration, while a short CC prevents residual trees from reaching the next diameter class, hindering volume recovery. Adjusting these metrics would better align harvesting practices with species growth dynamics and ecosystem resilience. However, implementing stricter criteria may conflict with local livelihood practices. Firewood collection remains the main energy source, typically involving small-diameter trees below the current MLD (CVS and INVEMAR 2010; Dupont et al. 2025). Recent surveys indicate that 94% of households use *R. mangle* for fuelwood, extracting intensively for up to 100 days per year (Dupont et al. 2025). Although essential for subsistence, this practice is a major anthropogenic driver of mangrove degradation (Chowdhury et al. 2017; Huxham et al. 2017).

Alternative strategies have proven successful elsewhere. In Saadani National Park, Tanzania, promoting alternative fuels among higher-income households reduced unsustainable harvesting while boosting incomes through enhanced shrimp fisheries (McNally et al. 2011). In Indonesia, the selective use of deadwood is permitted to satisfy firewood demand without cutting live trees (Mugi et al. 2022; Sillanpää et al. 2017). Nevertheless, further study is needed to evaluate the ecological effects of deadwood removal, given its role in nutrient cycling and habitat provision (Chisika and Yeom 2021; Wijas et al. 2024). In Cispatá Bay, similar approaches—including deadwood utilization, promotion of alternative fuels, and targeted application of silvicultural criteria for construction and commercialization—could reconcile conservation goals with community well-being.

The effectiveness of management plans depends not only on regeneration and recruitment but also on volume recovery after each rotation (Andrade et al. 2019; Schöngart 2008). To enhance regeneration, we recommend active planting in canopy gaps, as *R. mangle* seedlings perform best under open canopies (Ellison and Farnsworth 1993). Enrichment planting and controlled pruning can accelerate growth in *Rhizophora* species (Ferreira et al. 2015; Kathiresan et al. 2019). Similarly, crown liberation, widely used in managed tropical forests, can increase productivity and shorten the time needed to reach MDL while providing sustainable firewood (Grogan and Landis 2009). Given the high current density of *R. mangle* in Cispatá Bay, we recommend low-intensity harvesting that maintains large individuals essential for ecosystem services such as coastal protection, flood mitigation, and erosion control (Alongi 2008; Asari et al. 2021). To support this, the silvicultural thresholds proposed in this study provide science-sabed criteria that can guide the revision of local management plans and support updates to national forestry regulations for mangrove ecosystems. Achieving long-term sustainability, however, also requires active community participation, integration of socio-cultural needs, and adaptive monitoring of forest recovery to guide future interventions.

Conclusions

The integration of dendrochronological methods and biometric modeling has enabled the derivation of adjusted silvicultural parameters for *Rhizophora mangle* in Cispatá Bay, revealing substantial differences from the parameters currently employed. The findings indicate that the prevailing criteria may result in premature harvesting, thereby impeding forest recovery and threatening its sustainability.

The use of adjusted models that account for autocorrelation has enhanced the predictive capacity and physiological interpretation of growth parameters. Furthermore, the correction for eccentricity has served to reduce biases that are often overlooked in tropical studies. This positions the proposed methodology as a reference for adaptive management in mangroves with access or extraction restrictions.

However, the implementation of the revised criteria should be gradual process, supporting by ongoing monitoring, given the reliance of local communities on small-diameter timber resources. The transition to evidence-based management necessitates community involvement and the incorporation of their needs into the change process, with a particular focus on regeneration and equitable access to resources.

In summary, the study proposes a robust and scientifically based forest governance model that can be adapted to other species and regions prior to its experimental validation. In order to advance towards truly sustainable forestry in Caribbean mangroves and beyond, it is essential to embrace interdisciplinary collaboration, continuous monitoring, and the integration of social and ecological values.

Declarations

Acknowledgments

We gratefully acknowledge the Bosques y Cambio Climático Laboratory at the Department of Forest Sciences, National University of Colombia, for providing the necessary infrastructure and equipment for data processing. We also thank the University of Exeter, Fundación Omacha, the Corporación Autónoma Regional de los Valles del Sinú y del San Jorge (CVS), and the Instituto de Investigaciones Marinas y Costeras (INVEMAR) for their logistical support during fieldwork. We are especially thankful to INVEMAR for the provision of the forest inventory data and to the local community of San Antero for their permission to conduct this research in their territory.

Funding

This research was funded by the Universidad Nacional de Colombia (grant number 61083)

Competing interests

The authors declare that they have no known competing financial interests or personal

relationships that could have appeared to influence the work reported in this paper.

Author Contributions

All authors contributed to the study's conception and design. Material preparation and data collection were carried out by David Valderrama and Valeria Aguiar. Data analysis was conducted by David Valderrama and Sergio Orrego. The first draft of the manuscript was written by David Valderrama, and the final version was prepared by David Valderrama, Jaime Polanía, and Sergio Orrego. Jaime Polanía secured funding for the project, and both Jaime Polanía and Sergio Orrego supervised the research. All authors read and approved the final manuscript.

Data Availability

Tree-ring data used in this study are publicly available in the Mendeley Data repository at DOI: 10.17632/z42tbzp2n5.1. Forest inventory data are not publicly available as they are the property of a private organization and subject to restrictions.

References

1. Alongi DM (2008) Mangrove forests: Resilience, protection from tsunamis, and responses to global climate change. *Estuarine, Coastal and Shelf Science*, *76*(1), 1–13. https://doi.org/10.1016/j.ecss.2007.08.024
2. Andrade VHF, Machado SA, Figueiredo Filho A, Botosso PC, Miranda BP, Schöngart J (2019) Growth models for two commercial tree species in upland forests of the Southern Brazilian Amazon. *Forest Ecology and Management*, *438*, 215–223. https://doi.org/10.1016/j.foreco.2019.02.030
3. Asari N, Suratman MN, Mohd Ayob NA, Abdul Hamid NH (2021) Mangrove as a Natural Barrier to Environmental Risks and Coastal Protection. In *Mangroves: Ecology, Biodiversity and Management* (pp. 305–322). Springer. https://doi.org/10.1007/978-981-16-2494-0_13
4. Bhowmik AK, Padmanaban R, Cabral P, Romeiras, MM (2022) Global Mangrove Deforestation and Its Interacting Social-Ecological Drivers: A Systematic Review and Synthesis. *Sustainability*, *14*(8), Article 8. https://doi.org/10.3390/su14084433
5. Bimrah K, Dasgupta R, Hashimoto S, Saizen I, Dhyani S (2022) Ecosystem Services of Mangroves: A Systematic Review and Synthesis of Contemporary Scientific Literature. *Sustainability*, *14*(19), Article 19. https://doi.org/10.3390/su141912051
6. Bocking E, Cooper DJ, Price J (2017) Using tree ring analysis to determine impacts of a road on a boreal peatland. *Forest Ecology and Management*, *404*, 24–30. https://doi.org/10.1016/j.foreco.2017.08.007
7. Brienen RJW, Zuidema PA (2006) The use of tree rings in tropical forest management: Projecting timber yields of four Bolivian tree species. *Forest Ecology and Management*, *226*(1), 256–267. https://doi.org/10.1016/j.foreco.2006.01.038
8. Brienen RJW, Zuidema PA, During HJ (2006) Autocorrelated growth of tropical forest trees: Unraveling patterns and quantifying consequences. *Forest Ecology and Management*, *237*(1), 179–190. https://doi.org/10.1016/j.foreco.2006.09.042
9. Brienen RJW, Zuidema PA, Martínez-Ramos M (2010) Attaining the canopy in dry and moist tropical forests: Strong differences in tree growth trajectories reflect variation in growing conditions. *Oecologia*, *163*(2), 485–496. https://doi.org/10.1007/s00442-009-1540-5
10. Bunn A, Korpela M, Biondi F, Campelo F, Mérian P, Qeadan F, Zang C (2022) *dplR: Dendrochronology Program Library in R* [Computer software]. https://cran.r-project.org/package=dplR

11. Castellanos-Galindo GA, Casella E, Tavera H, Zapata Padilla LA, Simard M (2021) Structural Characteristics of the Tallest Mangrove Forests of the American Continent: A Comparison of Ground-Based, Drone and Radar Measurements. *Frontiers in Forests and Global Change*, *4*. https://doi.org/10.3389/ffgc.2021.732468
12. Chen R, Twilley RR (1998) A gap dynamic model of mangrove forest development along gradients of soil salinity and nutrient resources. *Journal of Ecology*, *86*(1), 37–51. https://doi.org/10.1046/j.1365-2745.1998.00233.x
13. Chisika SN, Yeom C (2021) Enhancing Ecologically Sustainable Management of Deadwood in Kenya's Natural Forests. *International Journal of Forestry Research*, *2021*(1), 6647618. https://doi.org/10.1155/2021/6647618
14. Chowdhury MdQ, Schmitz N, Verheydens A, Sass-Klaassen U, Koedam N, Beeckman H (2008) Nature and Periodicity of Growth Rings in two Bangladeshi Mangrove Species. *IAWA Journal*. https://doi.org/10.1163/22941932-90000185
15. Chowdhury MdQ, Kitin P, De Ridder M, Delvaux C, Beeckman H (2016) Cambial dormancy induced growth rings in Heritiera fomes Buch.- Ham.: A proxy for exploring the dynamics of Sundarbans, Bangladesh. *Trees*, *30*(1), 227–239. https://doi.org/10.1007/s00468-015-1292-2
16. Chowdhury RR, Uchida E, Chen L, Osorio V, Yoder L (2017) Anthropogenic Drivers of Mangrove Loss: Geographic Patterns and Implications for Livelihoods. In Rivera-Monroy VH, Lee SY, Kristensen RR, Twilley (Eds.), *Mangrove Ecosystems: A Global Biogeographic Perspective: Structure, Function, and Services* (pp. 275–300). Springer International Publishing. https://doi.org/10.1007/978-3-319-62206-4_9
17. Chowdhury MdQ, Sarker SK, Sultana R, Datta A, Saimun MdS, Rashid AZMM (2023a) Synergistic effects of climate and salinity on radial growth of *Excoecaria agallocha* L. in the Sundarbans world heritage mangrove ecosystem. *Estuarine, Coastal and Shelf Science*, *280*, 108181. https://doi.org/10.1016/j.ecss.2022.108181
18. Chowdhury MdQ, Sarker SK, Das Gupta A, Datta A (2023b) Radial growth in mangrove *Xylocarpus granatum* J. Koenig is driven by salinity in the Sundarbans, Bangladesh. *Dendrochronologia*, *79*, 126082. https://doi.org/10.1016/j.dendro.2023.126082
19. Chowdhury MdQ, Sarker SK, Marma M, Rahman MS, Datta A (2024) Climate and salinity together control above ground carbon accumulation in the Sundarbans mangrove ecosystem. *Ocean & Coastal Management*, *255*, 107242. https://doi.org/10.1016/j.ocecoaman.2024.107242
20. Cisneros-de la Cruz DJ, Martínez-Castillo J, Herrera-Silveira J, Yáñez-Espinosa L, Ortiz-García M, Us-Santamaria R, Andrade JL (2018) Short-distance barriers affect genetic variability of Rhizophora mangle L. in the Yucatan Peninsula. *Ecology and Evolution*, *8*(22), 11083–11099. https://doi.org/10.1002/ece3.4575
21. Conde MLG, Piedade MTF, Wittmann F, Nascimento RGM, Schöngart J (2024) Evaluation of the management potential of timber resources in clearwater floodplain forests in the Amazon using growth models. *Journal of Environmental Management*, *351*, 119781. https://doi.org/10.1016/j.jenvman.2023.119781
22. Coronado-Molina C, Day JW, Reyes E, Perez BC (2004) Standing crop and aboveground biomass partitioning of a dwarf mangrove forest in Taylor River Slough, Florida. *Wetlands Ecology and Management*, *12*(3), 157–164. https://doi.org/10.1023/B:WETL.0000034071.17156.c0
23. Corporación Autónoma Regional de los Valles del Sinú y del San Jorge (CVS), Instituto de Investigaciones Marinas y Costeras (INVEMAR) (2010) *Plan integral de manejo del Distrito de Manejo Integrado (DMI) bahía de Cispatá—La Balsa—Tinajones y sectores aledaños del delta estuarino del río Sinú, departamento de Córdoba.*
24. Cybis Elektronik, Data AB (n.d.-a) *CooRecorder* [Computer software]. http://www.cybis.se/forfun/dendro/
25. Cybis Elektronik, Data AB (n.d.-b) *CDendro* [Computer software]. https://www.cybis.se/forfun//dendro/index.htm
26. da Silva CRA, Santos-Silva M, Ferreira LMdS, Leite KRB, da Silva LB (2015) Morphological and anatomical aspects of the leaves of *Rhizophora mangle L*. (Rhizophoraceae) under different lighting conditions. *Journal of Neotrropical Biology*, *12*(2), 74–80. https://doi.org/10.5216/rbn.v12i2.33405
27. Dauber E, Fredericksen TS, Peña M (2005) Sustainability of timber harvesting in Bolivian tropical forests. *Forest Ecology and Management*, *214*(1), 294–304. https://doi.org/10.1016/j.foreco.2005.04.019

28. De Ridder M, Van den Bulcke J, Van Acker J, Beeckman H (2013) Tree-ring analysis of an African long-lived pioneer species as a tool for sustainable forest management. *Forest Ecology and Management*, *304*, 417–426. https://doi.org/10.1016/j.foreco.2013.05.007
29. Duke NC (2001) Gap creation and regenerative processes driving diversity and structure of mangrove ecosystems. *Wetlands Ecology and Management*, *9*(3), 267–279. https://doi.org/10.1023/A:1011121109886
30. Dupont R, Diallo K, Georis S, Kungula Makoso D, Ximenes AC, Satyanarayana B, Tarelkin Y, Diouf Goudiaby K, Hugé J, Polanía J, Dahdouh-Guebas F (2025) Species-Poor Mangrove Forests also Provide Rich Ecosystem Goods and Services. *Economic Botany*. https://doi.org/10.1007/s12231-024-09628-8
31. Ellison AM, Farnsworth EJ (1993) Seedling survivorship, growth, and response to disturbance in Belizean mangal. *American Journal of Botany*, *80*(10), 1137–1145. https://doi.org/10.1002/j.1537-2197.1993.tb15345.x
32. Estrada GCD, Callado CH, Soares MLG, Lisi CS (2008) Annual growth rings in the mangrove *Laguncularia racemosa* (Combretaceae). *Trees*, *22*(5), 663–670. https://doi.org/10.1007/s00468-008-0224-9
33. Ferreira AC, Ganade G, Luiz de Attayde J (2015) Restoration versus natural regeneration in a neotropical mangrove: Effects on plant biomass and crab communities. *Ocean & Coastal Management*, *110*, 38–45. https://doi.org/10.1016/j.ocecoaman.2015.03.006
34. Fichtler E, Clark DA, Worbes M (2003) Age and Long-term Growth of Trees in an Old-growth Tropical Rain Forest, Based on Analyses of Tree Rings and 14C1. *Biotropica*, *35*(3), 306–317. https://doi.org/10.1111/j.1744-7429.2003.tb00585.x
35. Free CM, Matthew Landis R, Grogan J, Schulze MD, Lentini M, Dünisch O (2014) Management implications of long-term tree growth and mortality rates: A modeling study of big-leaf mahogany (*Swietenia macrophylla*) in the Brazilian Amazon. *Forest Ecology and Management*, *330*, 46–54. https://doi.org/10.1016/j.foreco.2014.05.057
36. Gebrekirstos A, Mitlöhner R, Teketay D, Worbes M (2008) Climate–growth relationships of the dominant tree species from semi-arid savanna woodland in Ethiopia. *Trees*, *22*(5), 631–641. https://doi.org/10.1007/s00468-008-0221-z
37. Giraldo JA, del Valle JI (2011) Estudio del crecimiento de *Prioria copaifera* (Caesalpinaceae) mediante técnicas dendrocronológicas. *Revista de Biología Tropical*, *59*(4), 1813–1831.
38. Groenendijk P, van der Sleen P, Vlam M, Bunyavejchewin S, Bongers F, Zuidema PA (2015) No evidence for consistent long-term growth stimulation of 13 tropical tree species: Results from tree-ring analysis. *Global Change Biology*, *21*(10), 3762–3776. https://doi.org/10.1111/gcb.12955
39. Grogan J, Landis RM (2009) Growth history and crown vine coverage are principal factors influencing growth and mortality rates of big-leaf mahogany Swietenia macrophylla in Brazil. *Journal of Applied Ecology*, *46*(6), 1283–1291. https://doi.org/10.1111/j.1365-2664.2009.01720.x
40. Hussain SA, Badola R (2010) Valuing mangrove benefits: Contribution of mangrove forests to local livelihoods in Bhitarkanika Conservation Area, East Coast of India. *Wetlands Ecology and Management*, *18*(3), 321–331. https://doi.org/10.1007/s11273-009-9173-3
41. Huxham M, Dencer-Brown A, Diele K, Kathiresan K, Nagelkerken I, Wanjiru C (2017) Mangroves and People: Local Ecosystem Services in a Changing Climate. In *Mangrove Ecosystems: A Global Biogeographic Perspective: Structure, Function, and Services* (pp. 245–274). Springer International Publishing. https://doi.org/10.1007/978-3-319-62206-4_8
42. Inga JG, del Valle JI (2017) Log-relative growth: A new dendrochronological approach to study diameter growth in *Cedrela odorata* and *Juglans neotropica*, Central Forest, Peru. *Dendrochronologia*, *44*, 117–129. https://doi.org/10.1016/j.dendro.2017.03.009
43. Kathiresan K, Narendran R, Kalidasan K, Dinesh P (2019) Pruning of shoot branches: An efficient technique for stimulating the mangrove growth (*Rhizophora mucronata*). *Biocatalysis and Agricultural Biotechnology*, *17*, 309–312. https://doi.org/10.1016/j.bcab.2018.12.006
44. Kodikara KAS, Jayatissa LP, Huxham M, Dahdouh-Guebas F, Koedam N (2017) The effects of salinity on growth and survival of mangrove seedlings changes with age. *Acta Botanica Brasilica*, *32*, 37–46. https://doi.org/10.1590/0102-33062017abb0100

45. Kumari P, Pathak B (2023) Effect of Climate Change and Urbanization on Mangrove Ecosystem. In *Climate Change and Urban Environment Sustainability* (pp. 293–301). Springer Nature. https://doi.org/10.1007/978-981-19-7618-6_16
46. Lisboa VDP, Miranda DLCD, França LCDJ, Stepka TF, Condé TM, Venturoli F, Pesck VA, Watzlawick LF, Lisboa GDS. (2025) Minimum Diameter and Cutting Cycle of *Copaifera Langsdorffii* in Brazilian Neotropical Forest. *TreeDimensional*, *14*(42), 1–10. https://doi.org/10.55746/treed.2025.02.042
47. López L, Villalba R, Bravo F (2013) Cumulative diameter growth and biological rotation age for seven tree species in the Cerrado biogeographical province of Bolivia. *Forest Ecology and Management*, *292*, 49–55. https://doi.org/10.1016/j.foreco.2012.12.011
48. Lovelock CE, Krauss KW, Osland MJ, Reef R, Ball MC (2016) The Physiology of Mangrove Trees with Changing Climate. In Goldstein G, Santiago LS (Ed), *Tropical Tree Physiology: Adaptations and Responses in a Changing Environment* (pp. 149–179). Springer International Publishing. https://doi.org/10.1007/978-3-319-27422-5_7
49. Martínez CE, Orrego SA, Giraldo JA, del Valle JI, Hernández-Barajas F, David DA (2025) Autocorrelation as a critical factor of growth depensation of tropical trees in the Chocó biogeographic region. *Ecological Modelling*, *500*, 110949. https://doi.org/10.1016/j.ecolmodel.2024.110949
50. McNally CG, Uchida E, Gold AJ (2011) Biodiversity Conservation and Poverty Traps Special Feature: The effect of a protected area on the tradeoffs between short-run and long-run benefits from mangrove ecosystems. *Proceedings of the National Academy of Science*, *108*, 13945–13950. https://doi.org/10.1073/pnas.1101825108
51. Mehtätalo L, Lappi J (2020) *Biometry for Forestry and Environmental Data*. CRC Press. https://doi.org/10.1201/9780429173462
52. Méndez-Alonzo R, Moctezuma C, Ordoñez VR, Angeles G, Martínez AJ, López-Portillo J (2015) Root biomechanics in *Rhizophora mangle*: Anatomy, morphology and ecology of mangrove's flying buttresses. *Annals of Botany*, *115*(5), 833–840. https://doi.org/10.1093/aob/mcv002
53. Menezes M, Berger U, Worbes M (2003) Annual growth rings and long-term growth patterns of mangrove trees from the Bragança peninsula, North Brazil. *Wetlands Ecology and Management*, *11*(4), 233–242. https://doi.org/10.1023/A:1025059315146
54. Michaelis L, Menten ML (1913) Die Kinetik der Invertinwirkung. *Biochemische Zeitschrift*, *49*, 333–369.
55. Mitra A (2020) Ecosystem Services of Mangroves: An Overview. In *Mangrove Forests in India: Exploring Ecosystem Services* (pp. 1–32). Springer International Publishing. https://doi.org/10.1007/978-3-030-20595-9_1
56. Mugi LM, Kiss D, Kairo JG, Huxham MR (2022) Stocks and Productivity of Dead Wood in Mangrove Forests: A Systematic Literature Review. *Frontiers in Forests and Global Change*, *5*. https://doi.org/10.3389/ffgc.2022.767337
57. Ouyang X, Lee SY, Connolly RM (2017) The role of root decomposition in global mangrove and saltmarsh carbon budgets. *Earth-Science Reviews*, *166*, 53–63. https://doi.org/10.1016/j.earscirev.2017.01.004
58. Palacios ML, Cantera JR (2017) Mangrove timber use as an ecosystem service in the Colombian Pacific. *Hydrobiologia*, *803*(1), 345–358. https://doi.org/10.1007/s10750-017-3309-x
59. Pinheiro J, Bates D, DebRoy S, Sarkar D, R Core Team (2021) *nlme: Linear and Nonlinear Mixed Effects Models*. https://CRAN.R-project.org/package=nlme
60. R Core Team (2024) *R: A language and environment for statistical computing* (Version 4.1.1) [Computer software]. https://www.R-project.org/
61. Rahman MdS, Sass-Klaassen U, Zuidema PA, Chowdhury MdQ, Beeckman H (2020) Salinity drives growth dynamics of the mangrove tree *Sonneratia apetala* Buch. -Ham. In the Sundarbans, Bangladesh. *Dendrochronologia*, *62*, 125711. https://doi.org/10.1016/j.dendro.2020.125711
62. Ramírez-Correa JA, Molina-Grajales EC, Bernal-Escobar M (2010) Anillos anuales y clima en *Rhizophora mangle L*. de la bahía de Cispatá, Colombia. *Revista Facultad Nacional de Agronomía Medellín*, *63*(2), 5639–5650.

63. República de Colombia (1996) *Decreto 1791 de 1996: Régimen de aprovechamiento forestal persistente en bosques naturales*. https://www.funcionpublica.gov.co/eva/gestornormativo/norma.php?i=1296
64. Richards FJ (1959) A Flexible Growth Function for Empirical Use. *Journal of Experimental Botany*, *10*(2), 290–301. https://doi.org/10.1093/jxb/10.2.290
65. Roberts RW, Ruara WW (1967) *Lamu mangrove inventory: Part 1 and 2*. Spartan Air Services (Canada) & Forest Department, Ministry of Environment and Natural Resources, Nairobi, Kenya.
66. Schöngart J (2008) *G*rowth-*O*riented *L*ogging (GOL): A new concept towards sustainable forest management in Central Amazonian várzea floodplains. *Forest Ecology and Management*, *256*(1), 46–58. https://doi.org/10.1016/j.foreco.2008.03.037
67. Sherman R, Fahey T, Battles J (2000) Small-scale disturbance and regeneration dynamics in a neotropical mangrove forest. *Journal of Ecology*, *88*(1), 165–178.
68. Siddique MRH, Zuidema PA, Sass-Klaassen U, Chowdhury MdQ (2021) Ring width and vessel features of the mangrove *Excoecaria agallocha* L. depend on salinity in the Sundarbans, Bangladesh. *Dendrochronologia*, *68*, 125857. https://doi.org/10.1016/j.dendro.2021.125857
69. Šilhán K (2019) Tree-ring eccentricity in the dendrogeomorphic analysis of landslides – A comparative study. *CATENA*, *174*, 1–10. https://doi.org/10.1016/j.catena.2018.11.002
70. Sillanpää M, Vantellingen J, Friess DA (2017) Vegetation regeneration in a sustainably harvested mangrove forest in West Papua, Indonesia. *Forest Ecology and Management*, *390*, 137–146. https://doi.org/10.1016/j.foreco.2017.01.022
71. Simpson LT, Chapman SK, Simpson LM, Cherry JA (2023) Do global change variables alter mangrove decomposition? A systematic review. *Global Ecology and Biogeography*, *32*(11), 1874–1892. https://doi.org/10.1111/geb.13743
72. Souza BT, Estrada GCD, Soares MLG, Callado CH (2016) Occurrence of annual growth rings in *Rhizophora mangle* in a region with low climate seasonality. *Anais Da Academia Brasileira de Ciências*, *88*, 517–525. https://doi.org/10.1590/0001-3765201620150009
73. Speer JH (2010) *Fundamentals of Tree-ring Research*. University of Arizona Press.
74. Srinivasan B (2022) A guide to the Michaelis–Menten equation: Steady state and beyond. *The FEBS Journal*, *289*(20), 6086–6098. https://doi.org/10.1111/febs.16124
75. Suárez BES (2004) The Sinú river delta on the northwestern Caribbean coast of Colombia: Bay infilling associated with delta development. *Journal of South American Earth Sciences*, *16*(7), 623–631. https://doi.org/10.1016/j.jsames.2003.10.005
76. Urrego LE, Molina EC, Suárez JA (2014) Environmental and anthropogenic influences on the distribution, structure, and floristic composition of mangrove forests of the Gulf of Urabá (Colombian Caribbean). *Aquatic Botany*, *114*, 42–49. https://doi.org/10.1016/j.aquabot.2013.12.006
77. Urrego LE, Polanía J, Buitrago MF, Cuartas LF, Lema A (2009) Distribution of Mangroves Along Environmental Gradients on San Andrés Island (Colombian Caribbean). *Bulletin of Marine Science*, *85*(1), 27–43.
78. Vanclay JK (1994) *Modelling forest growth and yield: Applications to mixed tropical forests*. CAB International.
79. Verheyden A, Kairo JG, Beeckman H, Koedam N (2004) Growth Rings, Growth Ring Formation and Age Determination in the Mangrove *Rhizophora mucronata*. *Annals of Botany*, *94*(1), 59–66. https://doi.org/10.1093/aob/mch115
80. Visser H, van der Maaten-Theunissen M, Maaten EV (2023) BAI BAI bias – An evaluation of uncertainties in calculating basal area increments from cores. *Dendrochronologia*, *78*, 126066. https://doi.org/10.1016/j.dendro.2023.126066
81. von Bertalanffy L (1934) Untersuchungen über die Gesetzlichkeit des Wachstums. I. Allgemeine Grundlagen der Theorie. Mathematisch-physiologische Gesetzlichkeiten des Wachstums bei Wassertieren. *Wilhelm Roux' Archiv für Entwicklungsmechanik der Organismen*, *131*, 613–652.
82. Wijas BJ, Allison SD, Austin AT, Cornwell WK, Cornelissen JHC, Eggleton P, Fraver S, Ooi MKJ, Powell JR, Woodall CW, Zanne AE (2024) The Role of Deadwood in the Carbon Cycle: Implications for Models, Forest Management, and Future

Climates. *Annual Review of Ecology, Evolution, and Systematics*, *55*(Volume 55, 2024), 133–155. https://doi.org/10.1146/annurev-ecolsys-110421-102327

83. Xu H, Sun Y, Wang X, Fu Y, Dong Y, Li Y (2014) Nonlinear Mixed-Effects (NLME) Diameter Growth Models for Individual China-Fir (Cunninghamia lanceolata) Trees in Southeast China. *PLOS ONE*, *9*(8), e104012. https://doi.org/10.1371/journal.pone.0104012

Figures

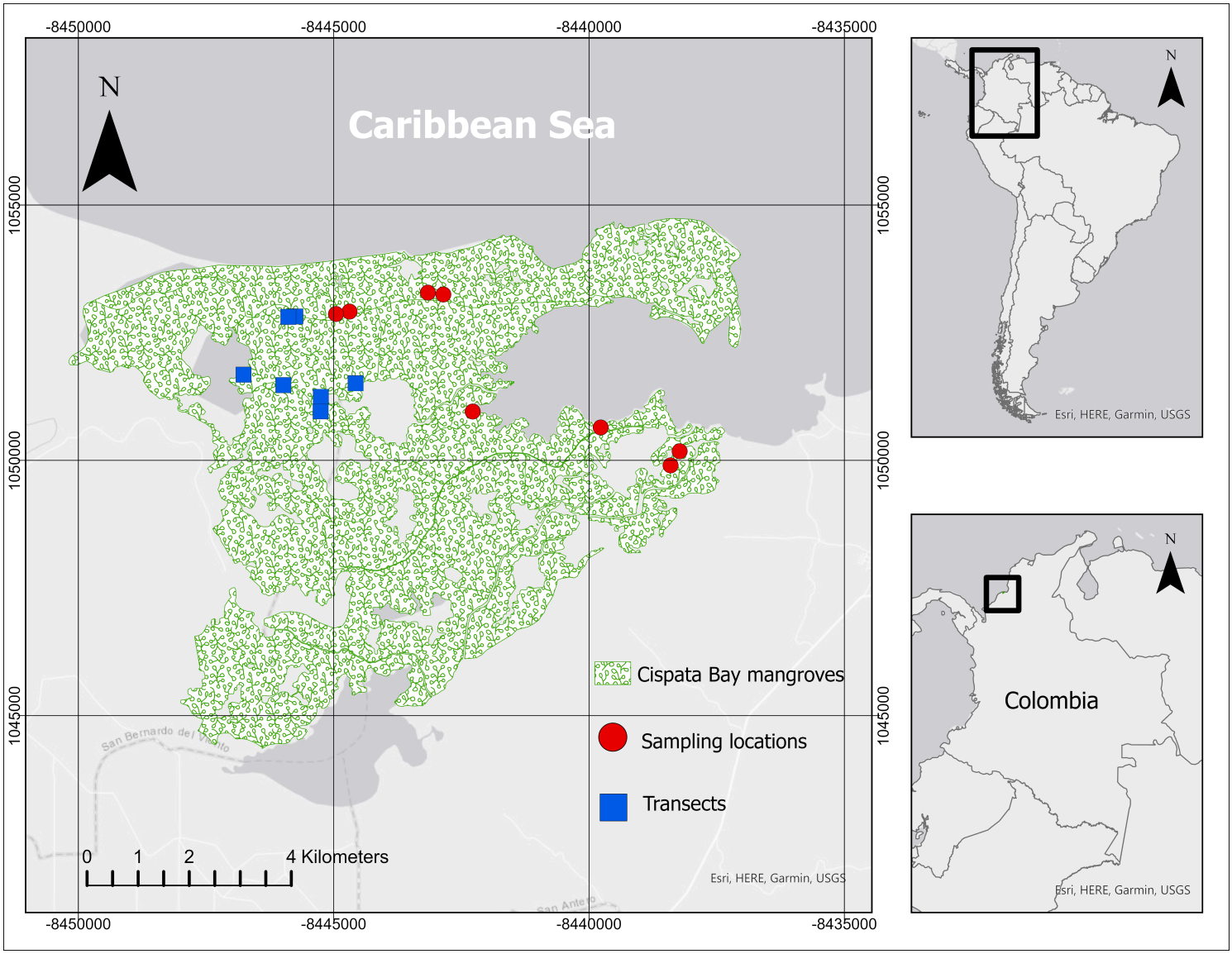

Figure 1

Location of the sampling sites and inventory transects in Cispatá Bay. Red dots represent the sampling locations where cross-sections were obtained. Blue squares are the locations of the forest inventory transects established during the formulation of the IMP by the INVEMAR (CVS & INVEMAR, 2010).

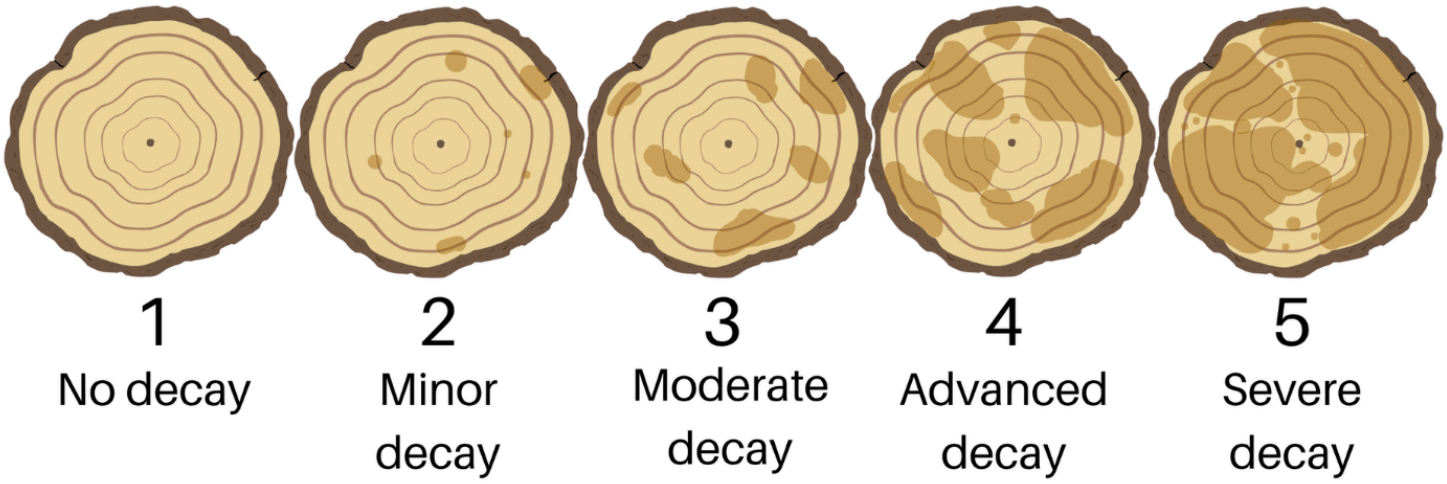

Figure 2

Graphical representation of the samples decay. (1) no decay, (2) minor decay, (3) moderate decay, (4) advanced decay, and (5) severe decay.

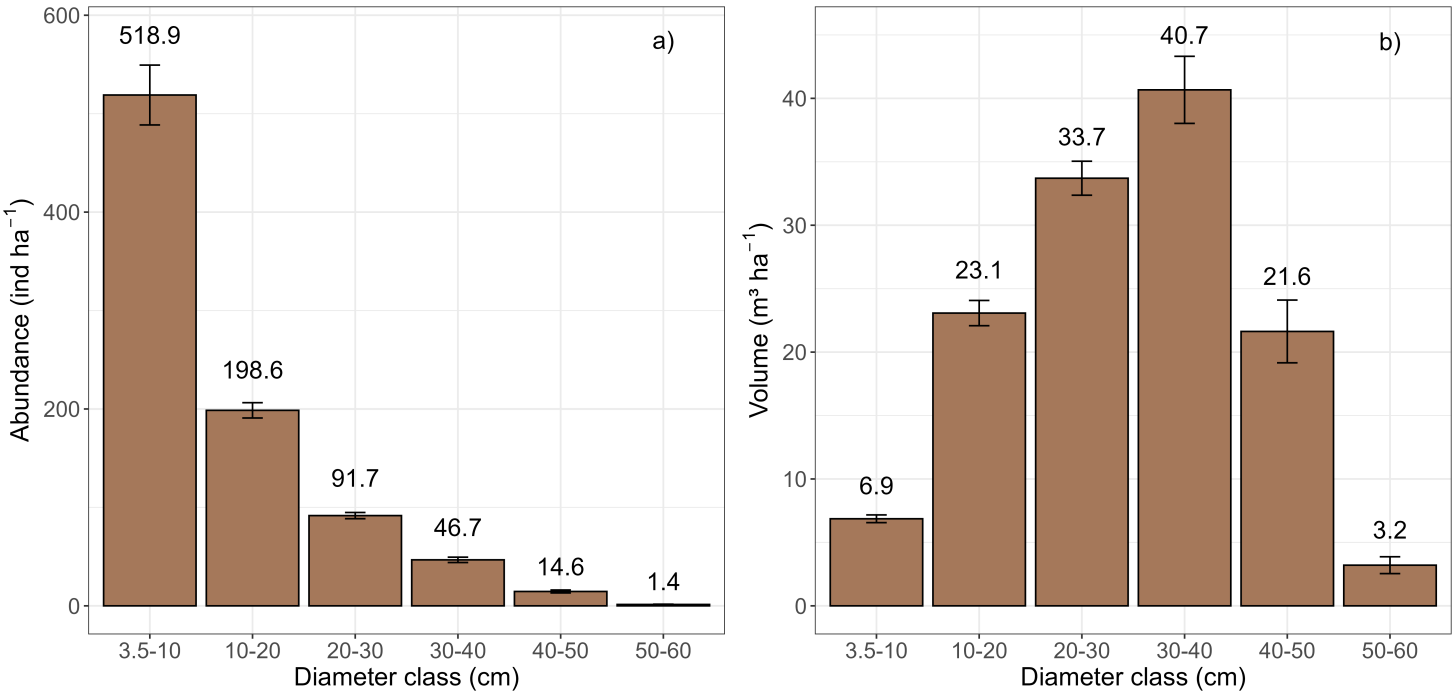

Figure 3

Rhizophora mangle density (a) and volume stock (b) distributions on diameter classes of 10 cm in Cispatá Bay. Bars' height represents the mean value, and whiskers the standard error.

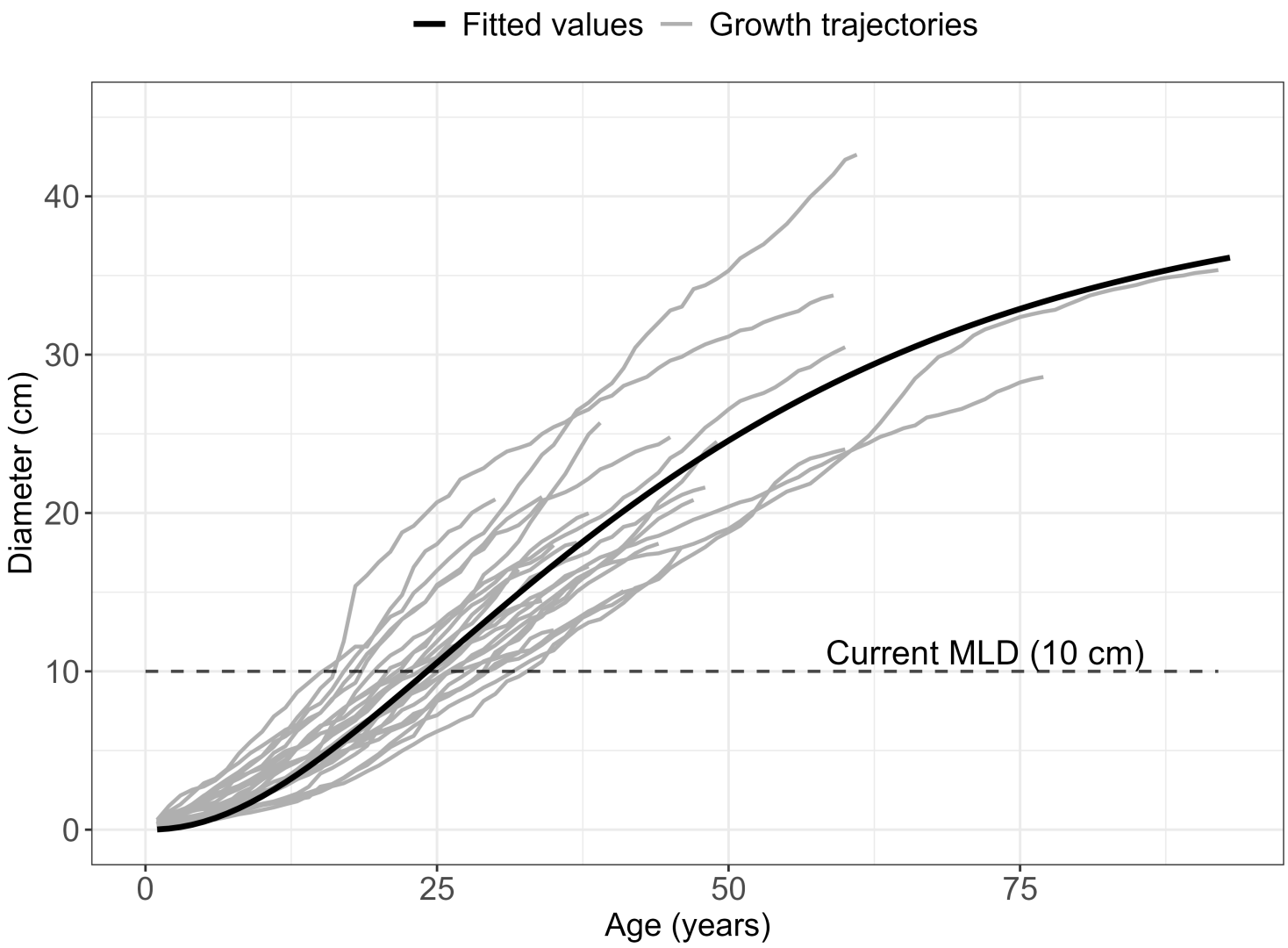

Figure 4

Fitted values of the von Bertalanffy model (1934; black) and diameter growth trajectories of *Rhizophora mangle*(grey). The dashed line represents the current minimum logging diameter (MLD) used in Cispatá Bay.

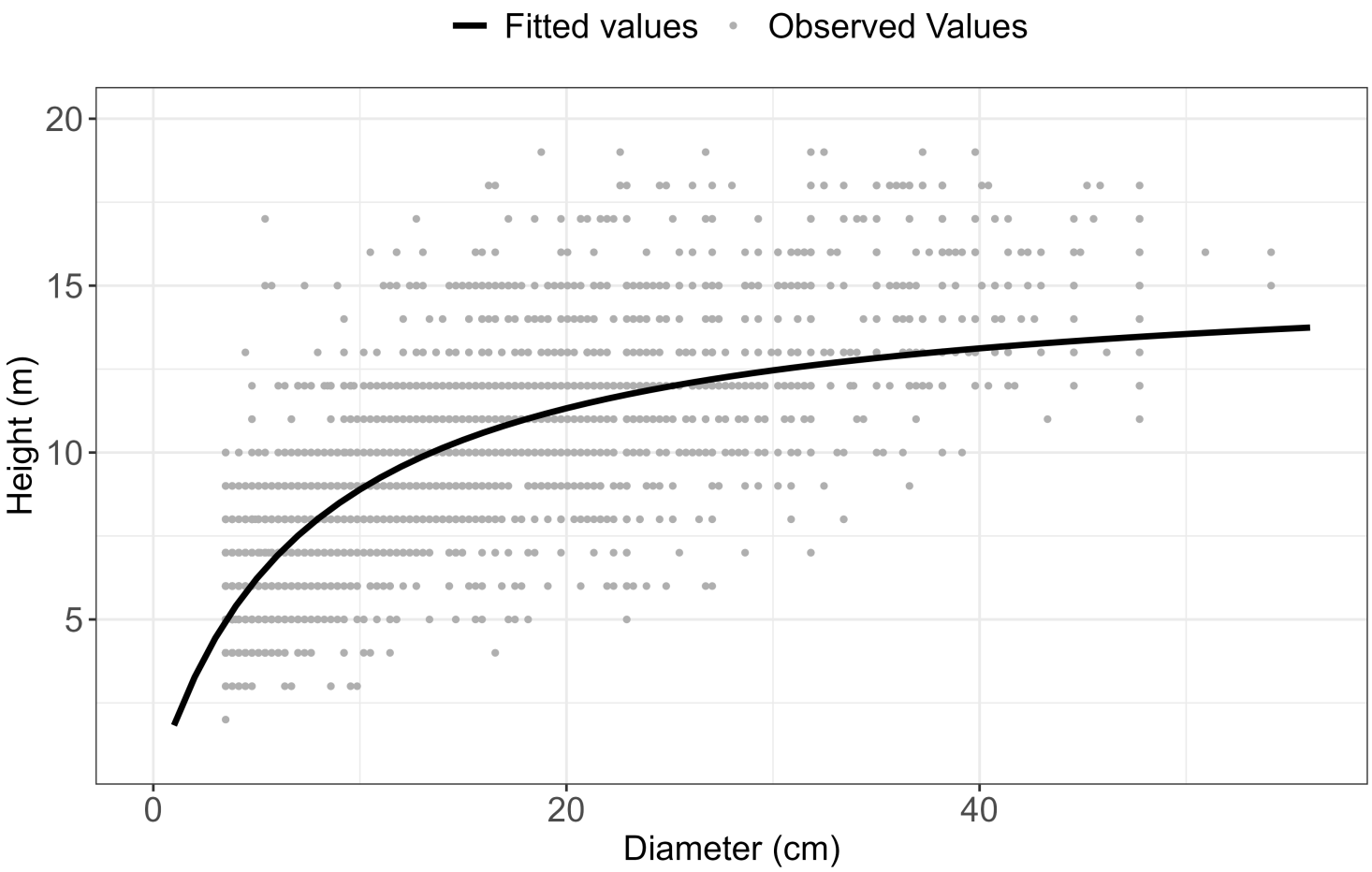

Figure 5

Diameter-height allometry and fitted values of the Michaelis-Menten (1913) model.

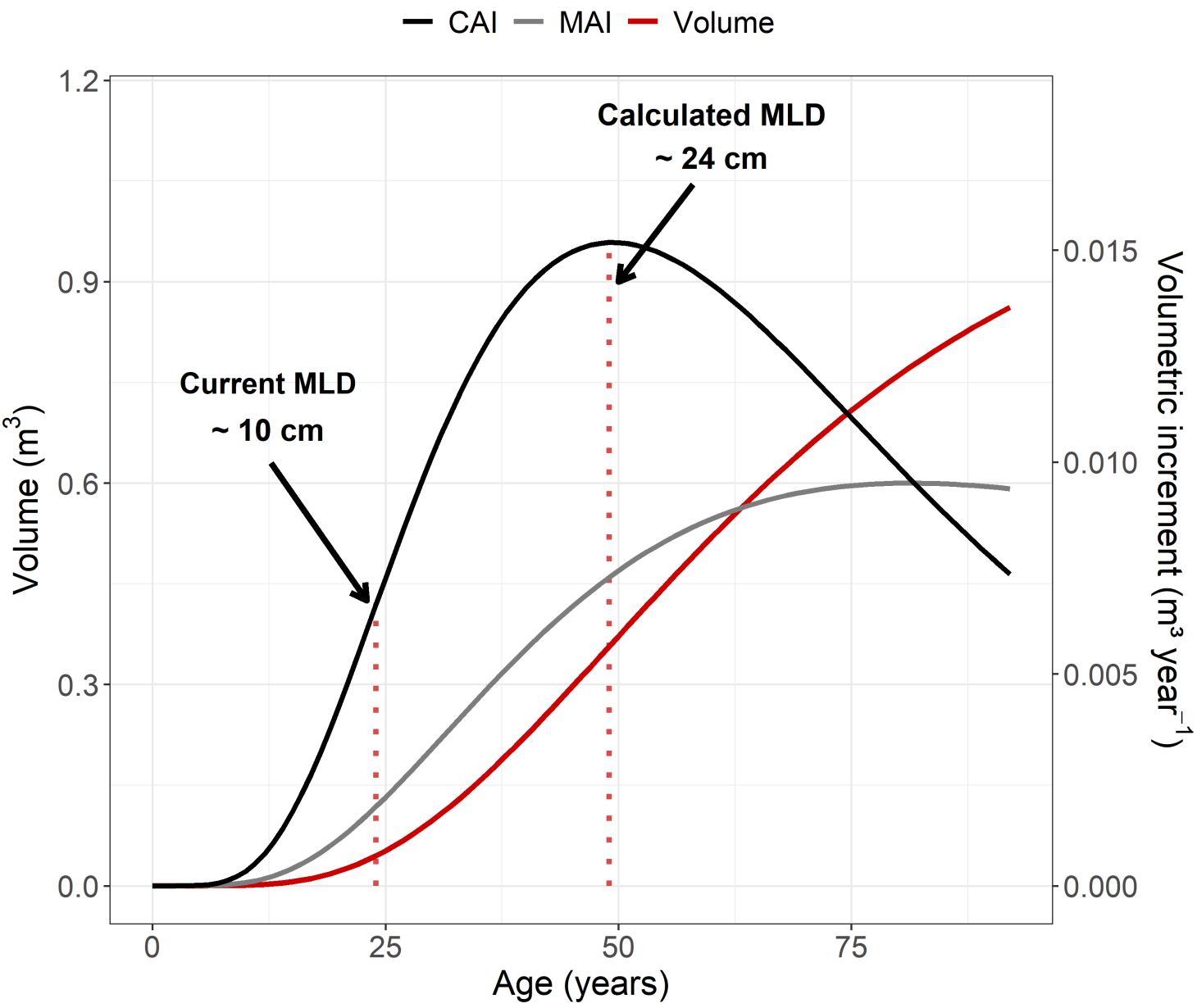

Figure 6

Mean cumulative volume growth (red), and current (CAIV; black) and mean (MAIV; grey) annual volume increments for *Rhizophora mangle*. Red dotted lines indicate the current and calculated minimum logging diameters (MLD) used in Cispatá Bay. The calculated MLD corresponds to the diameter attained at the age when CAIV reaches its maximum value

Supplementary Files

This is a list of supplementary files associated with this preprint. Click to download.

- Tables.docx
- Supplementarymaterial.docx